How does the Pinatubo eruption influence our understanding of long-term changes in ocean biogeochemistry?

Holly C. Olivarez[1,2], Nicole S. Lovenduski[2,3], Yassir A. Eddebbar[4], Amanda R. Fay[5], Galen A. McKinley[5], Michael N. Levy[6], Matthew C. Long[6]

[1]Department of Environmental Studies, University of Colorado, Boulder, CO, USA
[2]Institute of Arctic and Alpine Research, University of Colorado, Boulder, CO, USA
[3]Department of Atmospheric and Oceanic Sciences, University of Colorado, Boulder, CO, USA
[4]Scripps Institution of Oceanography, University of California San Diego, La Jolla, CA, USA
[5]Columbia University and Lamont-Doherty Earth Observatory, Palisades, NY, USA
[6]Climate and Global Dynamics Laboratory, National Center for Atmospheric Research, Boulder, Colorado, USA

Key Points:

- Using a large ensemble model, we quantify the impact of Pinatubo on observed, externally forced decadal changes in ocean biogeochemistry
- Nearly 100% of forced changes in apparent oxygen utilization and preindustrial carbon over 1993-2003 are attributable to Pinatubo
- Impacts of Pinatubo last several decades, affecting interpretation of anthropogenic changes from physical and biogeochemical observations

Corresponding author: Holly C. Olivarez, holly.olivarez@colorado.edu

Abstract

Pinatubo erupted during the first decadal survey of ocean biogeochemistry, embedding its climate fingerprint into foundational ocean biogeochemical observations and complicating the interpretation of long-term biogeochemical change. Here, we quantify the influence of the Pinatubo climate perturbation on externally forced decadal and multi-decadal changes in key ocean biogeochemical quantities using a large ensemble simulation of the Community Earth System Model designed to isolate the effects of Pinatubo, which cleanly captures the ocean biogeochemical response to the eruption. We find increased uptake of apparent oxygen utilization and preindustrial carbon over 1993-2003. Nearly 100% of the forced response in these quantities are attributable to Pinatubo. The eruption caused enhanced ventilation of the North Atlantic, as evidenced by deep ocean chlorofluorocarbon changes that appear 10-15 years after the eruption. Our results help contextualize observed change and contribute to improved constraints on uncertainty in the global carbon budget and ocean deoxygenation.

Plain Language Summary

Oceanographers' understanding of ocean properties comes from research cruises that take scientific measurements in the same locations every ten years. However, the first of these research cruises were deployed just after a large volcanic eruption in 1991 called Pinatubo. The eruption cooled the planet for several years, including the upper ocean. Here, we investigate how this eruption affected ocean properties using two collections of simulations of the Community Earth System Model which is a mathematical representation of the Earth system. The first collection of simulations shows the response to the eruption, while the second collection shows how ocean properties would have changed if there had been no eruption. The difference thus tell us the influence of the eruption on ocean properties. We find an increase of oxygen and preindustrial carbon over 1993-2003 due to Pinatubo, as well as an increase of ventilation of the North Atlantic that appears years after the eruption.

1 Introduction

Large volcanic eruptions have a dramatic impact on Earth's climate: sulfur aerosols from explosive eruptions interact with solar radiation, cooling Earth's surface [*Schneider et al.*, 2009]. The 1991 Pinatubo eruption injected approximately 20 megatons of sulfur dioxide into the stratosphere [*Robock*, 2000]. A massive aerosol cloud circled the globe in three weeks, reducing radiative forcing by $\sim$4.5 W m^{-2} (relative to typical forcing of 237 W m^{-2} reported in *Hansen et al.* [1992]), and producing a two-year reversal of the late 20^{th} century warming trend [*Robock*, 2000]. Beyond impacts on radiation and surface temperature, there is a need to quantify and understand how large-magnitude eruptions affect ocean biogeochemistry.

The first large-scale decadal survey of ocean biogeochemistry occurred in the years following the Pinatubo eruption [*Boyer et al.*, 2018]. Prior to 1991, the oceanographic community collected somewhere between zero and 1,000 hydrographic biogeochemical observations per year (Figure 1). From 1991-1996, however, the World Ocean Circulation Experiment (WOCE) and the Joint Global Ocean Flux Study (JGOFS) collected between 3,000 and 7,000 hydrographic biogeochemical observations per year [*Lauvset et al.*, 2022, see Figure 1]. As such, the climatic fingerprint of Pinatubo, which is pronounced in ocean circulation during this period [*Church et al.*, 2005; *Stenchikov et al.*, 2009], is likely embedded in the ocean biogeochemical observations from this key decadal survey.

Repeat hydrographic observations provide tremendous insight into the effects of anthropogenic climate change on ocean biogeochemistry. Observations collected via programs such as WOCE and JGOFS in the 1990s, the Climate and Ocean: Variability, Pre-

dictability and Change (CLIVAR) repeat hydrography program in the 2000s, and presently by the Global Ocean Ship-based Hydrographic Investigations Program (GO-SHIP) provide approximately decadal snapshots of ocean biogeochemical state along select transects in the Atlantic, Pacific, Indian, and Southern Ocean basins. Analysis of these observations provides a global assessment of decadal changes in measured biogeochemical quantities, such as nutrient, carbon, and oxygen concentrations, as well as in quantities inferred from physical and biogeochemical measurements, including apparent oxygen utilization (AOU; a measure of biological respiration and ocean circulation), anthropogenic carbon, and ocean circulation (inferred from measurements of, e.g., chlorofluorocarbons or CFCs). Using repeat hydrographic survey data, *Wanninkhof et al.* [2010] report large changes in AOU between 1989 and 2005 in the interior Atlantic basin, and *Johnson and Gruber* [2007] indicate that ocean ventilation changes are responsible for observed decadal AOU variability here. Similarly, *Deutsch et al.* [2006] attribute the large AOU variability in the interior Pacific basin in part to changes in ventilation. *Gruber et al.* [2004], *Sabine et al.* [2008], and *Gruber et al.* [2019] base their estimates of decadal changes and regional patterns of anthropogenic carbon storage by comparing sections from decadal hydrographic surveys. Finally, multiple studies based on hydrographic CFC data conclude that Southern Ocean meridional overturning accelerated from the 1990s to the 2000s [*Waugh et al.*, 2013; *Tanhua et al.*, 2013; *Ting and Holzer*, 2017]. The effects of Pinatubo on ocean circulation and biogeochemistry are likely woven into these findings, but have so far remained largely unexplored.

Modeling studies find that volcanic eruptions can affect change in ocean biogeochemistry. *Frölicher et al.* [2009] use a small ensemble of simulations in Climate System Model version 1.4 to examine the influence of large volcanic eruptions; they find that ocean oxygen inventory increases globally in the top 500m and that the perturbation persists for up to a decade post-eruption. In a separate study with the same model, *Frölicher et al.* [2011] find that the ocean carbon-climate feedback parameter is affected by large eruptions for up to 20 years. *Eddebbar et al.* [2019] use the Community Earth System Model-1 (CESM1) Large Ensemble and the Geophysical Fluid Dynamics Laboratory Earth System Model (ESM2M) Large Ensemble to investigate the physical and biogeochemical ocean response to tropical eruptions throughout the 20^{th} century; they find a large uptake of oceanic oxygen and carbon driven by a complex ocean physical response to volcanic perturbations, with important implications for attributing decadal variability in the ocean carbon sink. *McKinley et al.* [2020] find that Pinatubo drove a pronounced global ocean carbon uptake anomaly that peaked in 1992-1993. *Fay et al.* [2023] further isolate the effects of Pinatubo on key biogeochemical properties and show oxygen in the ocean interior permanently increases by 60 Tmol and ocean carbon uptake increases by 0.29 $\pm$0.14 Pg yr^{-1} in 1992 with pronounced changes in the deep ocean for oxygen and upper 150 m for carbon. Taken together, these studies suggest that Pinatubo had a substantial influence on ocean biogeochemical distributions and cycling, and insinuate that the reported, hydrography-based decadal and multi-decadal changes in ocean biogeochemistry may be influenced by the Pinatubo eruption.

Here, we investigate the impact of the Pinatubo eruption on decadal to multi-decadal changes in ocean biogeochemical properties using two ensembles of simulations from a state-of-the-art Earth system model. The simulations were designed to explicitly isolate the externally forced response of the Earth system due to Pinatubo: the first ensemble simulates the period from 1991 to 2025 under historical forcing, and the second ensemble is identical to the first but excludes the 1991 Pinatubo eruption [*Fay et al.*, 2023]. The difference in the respective ensemble means allows us to cleanly capture the forced response due to the eruption in the presence of internal variability and anthropogenic forcing, while the inter-ensemble spread captures the extent of the internal variability in the climate system. We sample the simulated ocean at the times and locations of the ocean hydrographic observation programs to reveal long-term biogeochemical changes associated with the Pinatubo climate perturbation. Our results help contextualize ob-

served changes in AOU, preindustrial and anthropogenic carbon, and chlorofluorocarbon-12 due to internally generated versus externally driven climate variability associated with volcanic eruptions, and contribute to improved constraints on uncertainty in the global carbon budget and ocean deoxygenation.

2 Methods

Our primary numerical tool is the Community Earth System Model version 1 (CESM1), a fully coupled climate model that simulates Earth's climate system [*Hurrell et al.*, 2013]. Four component models that each simultaneously simulate Earth's atmosphere, ocean, land, and sea ice are coupled with one central component that exchanges fluxes and boundary conditions between the individual components [*Danabasoglu et al.*, 2012; *Holland et al.*, 2012; *Hunke and Lipscomb*, 2008; *Lawrence et al.*, 2012]. The ocean component in CESM1 is named the Parallel Ocean Program version 2 [POP2; *Smith et al.*, 2010]. The model is defined at approximately 1° horizontal resolution and 60 vertical levels. Ocean carbon biogeochemistry is simulated using the ocean Biogeochemical Elemental Cycling (BEC) model, which is coupled to POP2. BEC includes full carbonate system and lower level trophic ecosystem dynamics, allowing for computation of inorganic carbon chemistry, oceanic pCO_2, air-to-sea CO_2 and O_2 fluxes, and a dynamic iron cycle that reflect physical transport, solubility variations, net community production, and ocean-atmosphere exchange [*Moore et al.*, 2013].

We analyze output from two sets of large initial-condition ensemble simulations conducted with CESM1. The first is a 29-member replicate of the CESM1 Large Ensemble [*Kay et al.*, 2015] for 1990-2025 conducted on the NCAR Cheyenne supercomputer [herein referred to as 'LENS'; *Fay et al.*, 2023]. Each ensemble member is forced identically but initialized with a slight modification to surface air temperature, producing an ensemble spread that reflects the influence of internal variability on the simulated Earth system response to Pinatubo. Recently, a second set of 29 ensemble members were generated that are identical to LENS but excluded the radiative forcing of Pinatubo eruption by removing the volcanic aerosol mass mixing ratio values for January 1991 to December 1995 and replacing them with values from a time when no large volcanic eruptions took place, January 1986 to December 1990 [herein referred to as 'NoPin'; *Fay et al.*, 2023].

Both ensembles compute carbonate chemistry using two different prescribed atmospheric CO_2 boundary conditions: 284.7 parts per million (ppm, from which we derive preindustrial dissolved inorganic carbon concentrations), and time-evolving observed historical and projected Representative Concentration Pathway 8.5 atmospheric CO_2 (from which we derive contemporary carbon concentrations). Anthropogenic carbon concentration is calculated by difference between the contemporary and preindustrial concentrations.

The ensembles are forced with prescribed atmospheric CFC-12 from 1990 to 2005. Modeled ocean CFC-12 concentrations were converted to pCFC-12 using the standard solubility formulation [*Warner and Weiss*, 1985]. We also make use of ideal age, an idealized passive model tracer that records the length of time since a parcel of water was last in contact with the atmosphere at the ocean surface [*Lester et al.*, 2020]. Since ideal age does not have atmospheric time-varying history, it is used to explore temporal changes in ocean circulation.

In this manuscript, we present the difference in the LENS and NoPin ensemble means, which isolates the modeled ocean biogeochemical anomalies associated with the Pinatubo eruption. We also present the standard deviation across the ensemble members as representative of internal variability. We use January to December values for the annual means in 1993 and 2003. The difference between the LENS and NoPin ensemble means (X) is

considered statistically significant at the 95% confidence interval if its ratio with the cross-ensemble standard deviation (σ) is greater than 2 divided by the square root of the degrees of freedom [N - 1, here N = 29; *Deser et al.*, 2012; *Fay et al.*, 2023],

$$\frac{X}{\sigma} \geq \frac{2}{\sqrt{N-1}}. \tag{1}$$

We subsample the model at the approximate locations of observed GO-SHIP hydrographic sections that, when taken together, follow the path of the global ocean thermohaline circulation [map inset, Figure 2; *Sarmiento and Gruber*, 2006]. In the Atlantic, we subsample a single meridional section along 25°W (akin to A16N, *Baringer and Bullister* [2013] and A16S, *Wanninkhof and Barbero* [2014]). In the Southern Ocean, we subsample along 63°S between 29 and 80°E (akin to S04I, *Rosenberg* [2006]) and along 67°S between 159°E and 73°W (akin to S04P, *Macdonald* [2018]). In the Pacific, we subsample a single meridional section along 150°W (akin to P16S, *Talley* [2014] and P16N, *Macdonald and Mecking* [2015]).

3 Results

A substantial fraction of the externally forced change in AOU that occurs from 1993 to 2003 along the path of the global ocean thermohaline circulation and across each basin can be attributed to Pinatubo (Figures 2 and S2). In the subpolar north and subtropical north and south Atlantic, LENS produces large (∼10 mmol m^{-3}), externally forced increases in AOU from 1993 to 2003 in waters with potential density ≥ 26.5 kg m^{-3} (Figure 2, top). The difference between the LENS and NoPin ensemble mean AOU changes (Figure 2, bottom) reveals a remarkable similarity to the LENS ensemble mean AOU changes (cf. Figure 2 top and bottom), indicating that Pinatubo is the main driver of externally forced decadal increases in AOU in the subpolar north and subtropical Atlantic. In the Pacific, the externally forced decadal change in AOU is more complex, with decreases in AOU in the northern subpolar region (isopycnal range 26-27 kg m^{-3}) and in the upper tropical thermocline(isopycnal range 23-26 kg m^{-3}; Figure 2, top). Again, the LENS ensemble mean AOU changes here are remarkably similar in magnitude and sign to the difference between the LENS and NoPin ensemble mean AOU changes (cf. Figure 2 top and bottom), indicating that Pinatubo played an important role in driving these forced AOU changes. Anomalies south of 40°S are mostly weak or statistically insignificant, suggesting weaker Pinatubo effects on AOU in this region. These externally forced, decadal changes in AOU occur in the presence of substantial internal variability that can enhance or diminish ensemble mean trends (Figure S1). For example, positive value increases in AOU beyond those of the ensemble mean (11 mmol m^{-3}) are exhibited in ensemble member 21 in the Atlantic transect (14.25 mmol m^{-3}), ensemble member 2 along the Indian transect in the Southern Ocean (13 mmol m^{-3}), and ensemble member 10 along the Pacific transect (18 mmol m^{-3}, see Figure S1).

In contrast to AOU, Pinatubo's eruption has little-to-no effect on the externally forced evolution of the interior ocean anthropogenic carbon distribution (Figure 3; corresponding zonal mean in Figure S3). Most of the change over 1993-2003 occurs in the subtropical thermocline in both basins, with additional anthropogenic carbon accumulation below 1000 m in the subpolar North Atlantic (approximately 40°N to 60°N). LENS ensemble mean anthropogenic carbon increases by as much as 10.25 mmol m^{-3} between 1993 and 2003, with marked increases in the Atlantic within the isopycnal range 24-27 kg m^{-3}, Southern Ocean along σ=27 kg m^{-3}, and Pacific within 23-26 kg m^{-3} (Figure 3, top). The difference between the LENS and NoPin ensemble mean anthropogenic carbon changes over 1993 to 2003 is an order of magnitude less than the LENS ensemble mean changes (cf. Figure 3 top and second rows), suggesting that Pinatubo does not influence the externally forced increase in interior ocean anthropogenic carbon.

Conversely, nearly all of the externally forced change in preindustrial carbon (carbon not directly affected by rising atmospheric CO_2) from 1993 to 2003 is attributable to Pinatubo's eruption (Figure 3; corresponding zonal mean in Figure S5). The largest changes in LENS preindustrial carbon also occur in the subtropical thermocline in both basins, and closely correspond in sign and magnitude to the changes attributable to Pinatubo over this period (cf. Figure 3 bottom two rows). This externally forced, decadal change in preindustrial carbon occurs amidst a backdrop characterized by high internal variability (Figure S5), yet the signal of Pinatubo emerges in the ensemble mean (Figure S5) and is statistically significant at the 95% confidence interval throughout much of the top 300m. Pinatubo thus acts to increase preindustrial carbon in the Atlantic pycnocline and decrease preindustrial carbon in the Pacific pycnocline when sampling the model along our selected cruise path, however zonal mean decadal changes due to Pinatubo are more muted, reflecting zonally complex changes in preindustrial carbon distributions associated with Pinatubo (cf. Figures 3 and S5).

Pinatubo has had long-lasting impacts on the deep North Atlantic, as evidenced by changes in the pCFC-12 distribution (Figure 4, Figure S7). While a 1995 virtual survey reflects little impact of Pinatubo on pCFC-12 in the deep North Atlantic, by the year 2000 there is a statistically significant 10-20 parts per trillion (ppt) decrease in pCFC-12 in the upper 1000 m over 35-60°N that persists through 2005, and a corresponding increase in pCFC-12 from 1000 m to the seafloor in the same region, (Figure 4, Figure S6). Ideal age shows similar Pinatubo-driven changes in the deep North Atlantic that extend through 2025 (Figure S7, Figure S8; see Methods for an explanation of ideal age). Taken together, these figures imply that Pinatubo affected North Atlantic ventilation, driving perturbations in water mass properties that persisted for many decades after the eruption.

4 Conclusions and Discussion

Our study uses an ensemble of Earth system model simulations to examine the spatiotemporal response of ocean biogeochemistry to the 1991 Pinatubo eruption amid internal climate variability, and to estimate the fingerprint of the Pinatubo climate perturbation in the hydrographic observational record. We find that the effects of the Pinatubo eruption manifest more strongly for some ocean biogeochemical variables than others: externally driven decadal changes in AOU and preindustrial carbon are strongly affected by the eruption, while changes in anthropogenic carbon show no discernible response to the eruption. We also find that the eruption has had long-lasting impacts on deep North Atlantic transient tracer distributions.

By investigating the externally forced (ensemble mean) evolution of multiple ocean variables in the decade following the eruption, we can begin to understand how Pinatubo altered key tracers of physical and biogeochemical processes. Pinatubo drove decadal-scale increases in both AOU and preindustrial carbon in the subtropical Atlantic thermocline, likely as a result of post-eruption cooling and solubility driven increases in dissolved oxygen and carbon [*Fay et al.*, 2023]. Pinatubo's cooling also drove increases in North Atlantic ventilation [*Fay et al.*, 2023], affecting pCFC-12 below the main thermocline for multiple decades. In the Pacific, CESM responds to the Pinatubo climate perturbation by producing El Niño-like conditions [*Eddebbar et al.*, 2019; *Fay et al.*, 2023]. This causes reduced upwelling of carbon-rich and oxygen-poor waters, reducing both AOU and preindustrial carbon concentrations.

One of the key findings from this study is that, while the Pinatubo climate perturbation influences the distribution of preindustrial carbon, it has no discernible impact on the externally forced changes in the anthropogenic carbon distribution. This finding agrees with previous studies that find an important role for Pinatubo in preindustrial carbon variability [*Eddebbar et al.*, 2019; *McKinley et al.*, 2020; *Fay et al.*, 2023],

and gives us additional confidence that observation-based estimates of changing anthropogenic carbon distribution [e.g., *Gruber et al.*, 2019]; [also *Müller, Jens Daniel, Gruber, Nicolas, Carter, Brendan R., Feely, et al., Decadal Trends in the Oceanic Storage of Anthropogenic Carbon from 1994 to 2014, in preparation for Authorea*] are relatively unaffected by the Pinatubo climate perturbation. This confidence, however, is only valid to the extent that the methods employed can accurately separate anthropogenic carbon from the much larger preindustrial component.

Repeat hydrographic observations of physical and biogeochemical ocean properties are a powerful tool for quantifying and diagnosing change in the real ocean, but one must exercise caution when attributing observed change to externally forced processes such as anthropogenic climate warming. Our study uses two ensembles of simulations from an Earth system model to explicitly isolate the role of (1) anthropogenic climate change and the Pinatubo climate perturbation (LENS ensemble mean), (2) anthropogenic climate change alone (NoPin ensemble mean), and by difference (3) the Pinatubo climate perturbation alone (LENS ensemble mean minus NoPin ensemble mean) in the temporal evolution of these properties. In this framework, the real world hydrographic observations represent a single ensemble member in LENS, wherein change over time is affected by internal climate variability, anthropogenic climate change, and the Pinatubo climate perturbation. Our approach thus helps to disentangle the drivers of change in the observed record, and points to an important role for Pinatubo.

Results from our study align with those reported in others studies on the decadal impacts of volcanic eruptions on ocean biogeochemistry. We find a zonal-mean increase in the oxygen content in the upper 300 m in the decade following the eruption across the Atlantic and Pacific sectors, consistent with *Frölicher et al.* [2009], who report post-eruption global oxygen increases in the upper 500 m and *Eddebbar et al.* [2019] who report anomalous ocean oxygen uptake immediately following the eruption with long lasting effects on subsurface distributions [*Fay et al.*, 2023].

Our findings come with several caveats. First, the horizontal resolution of our model is coarser (∼100 km) than the typical distance between hydrographic measurements (∼20 km). As such, our model sub-sampling exercise produces an estimate of biogeochemical properties averaged over multiple hydrographic stations, and parameterizes the small scale variations in biogeochemical properties captured by the observations. Second, the micro-nutrients contained in volcanic ash have been shown to impact carbon cycling [*Hamme et al.*, 2010; *Langman et al.*, 2010]; ash is not simulated in this experiment. Finally, several studies have commented on the ability to capture the externally forced signal from a medium-sized model ensemble [*Milinski et al.*, 2020]. Thus, our experiment with 29 ensemble members may not represent the true response of the modeled ocean biogeochemistry to the Pinatubo climate perturbation.

Despite these caveats, our novel experiment allows for quantification of the impact of the Pinatubo climate perturbation on observed decadal changes in ocean biogeochemistry. We show that the impacts of the Pinatubo eruption extend for several decades in the ocean, affecting interpretation of anthropogenic changes from physical and biogeochemical observations and illustrating a need to reference Pinatubo in the interpretation of observed water property changes. Because the highest numbers of ocean biogeochemical observations collected from hydrographic cruises through the WOCE/JGOFS [*Boyer et al.*, 2018] were immediately following a large, explosive volcanic eruption (1992 to 1996; Figure 1), it is logical that our understanding of long-term changes in ocean biogeochemistry has been influenced by the eruption's impacts. Our work adds to the growing body of literature suggesting that the Pinatubo climate perturbation caused large changes in ocean biogeochemical properties [*Frölicher et al.*, 2009; *Eddebbar et al.*, 2019; *McKinley et al.*, 2020; *Fay et al.*, 2023], and contributes to improved constraints on uncertainty in the global carbon budget and ocean deoxygenation.

Acknowledgments

Data were collected and made publicly available by the International Global Ship-based Hydrographic Investigations Program (http://www.go-ship.org/) and the national programs that contribute to it. We would like to acknowledge high-performance computing support from Cheyenne (https://doi.org/10.5065/D6RX99HX) provided by NCAR's Computational and Information Systems Laboratory, sponsored by the National Science Foundation. This material is based upon work supported by the National Center for Atmospheric Research, which is a major facility sponsored by the National Science Foundation under Cooperative Agreement No. 1852977. We are grateful for support from the National Science Foundation (OCE-1752724, OCE-1948624, OCE-1948664, OCE-1948728, AGS-2019625, OCE 1948599, and the Graduate Research Fellowship Program). This work benefited from computational assistance from R. X. Brady. We acknowledge the previous work done by the CESM Large Ensemble Community Project.

Data Availability Statement: The CESM source code is freely available at http://www2.cesm.ucar.edu. The model outputs described in this paper can be accessed at www.earthsystemgrid.org. The code used to generate the main text figures can be found on Zenodo at https://doi.org/10.5281/zenodo.8145484.

References

Baringer, M., and J. Bullister (2013), Cruise Report: A16N, *Ronald H. Brown*, *A16N*(2013 AUG 03-2013 OCT 03), https://cchdo.ucsd.edu/cruise/33RO20130,803.

Boyer, T., O. Baranova, C. Coleman, H. Garcia, A. Grodsky, R. Locarnini, A. Mishonov, C. Paver, J. Reagan, D. Seidov, I. Smolyar, K. Weathers, and M. Zweng (2018), *World Ocean Database 2018*, A. V. Mishonov, Technical Editor, NOAA Atlas NESDIS 87.

Church, J. A., N. J. White, and J. M. Arblaster (2005), Significant decadal-scale impact of volcanic eruptions on sea level and ocean heat content, *Nature*, *438*, 74–77, doi:https://doi.org/10.1038/nature04237.

Danabasoglu, G., S. C. Bates, B. P. Briegleb, S. R. Jayne, M. Jochum, W. G. Large, S. Peacock, and S. G. Yeager (2012), The CCSM4 Ocean Component, *J. Climate*, *25*, 1361–1389, doi:https://doi.org/10.1175/JCLI-D-11-00091.1.

Deser, C., A. Phillips, V. Bourdette, and H. Teng (2012), Uncertainty in climate change projections: the role of internal variability, *Clim. Dynam.*, *38*, 527–546, doi:https://doi.org/10.1007/s00382-010-0977-x.

Deutsch, C., S. Emerson, and L. Thompson (2006), Physical-biological interactions in north pacific oxygen variability, *Journal of Geophysical Research: Oceans*, *111*(C09S90), doi:https://doi.org/10.1029/2005JC003179.

Eddebbar, Y. A., K. B. Rodgers, M. C. Long, A. C. Subramanian, S.-P. Xie, and R. F. Keeling (2019), El Niño–like physical and biogeochemical ocean response to tropical eruptions, *J. Climate*, *32*(9), 2627–2649, doi: http://dx.doi.org/10.1175/JCLI-D-18-0458.1.

Fay, A. R., G. A. McKinley, N. S. Lovenduski, Y. Eddebbar, M. N. Levy, M. C. Long, H. C. Olivarez, and R. R. Rustagi (2023), Immediate and long-lasting impacts of the mt. pinatubo eruption on ocean oxygen and carbon inventories, *Global Biogeochemical Cycles*, *37*(2), e2022GB007,513, doi: https://doi.org/10.1029/2022GB007513, e2022GB007513 2022GB007513.

Frölicher, T. L., F. Joos, G.-K. Plattner, M. Steinacher, and S. C. Doney (2009), Natural variability and anthropogenic trends in oceanic oxygen in a coupled carbon cycle–climate model ensemble, *Global Biogeochem. Cycles*, *GB1003*, doi: http://dx.doi.org/10.1029/2008GB003316.

Frölicher, T. L., F. Joos, and C. C. Raible (2011), Sensitivity of atmospheric CO_2 and climate to explosive volcanic eruptions, *Biogeosciences*, *8*, 2317–2339, doi:

https://doi.org/10.5194/bg-8-2317-2011.

Gruber, N., P. Friedlingstein, C. B. Field, R. Valentini, M. Heimann, J. E. Richey, P. Romero-Lankao, D. Schulze, and C.-T. A. Chen (2004), The vulnerability of the carbon cycle in the 21st century: An assessment of carbon-climate-human interactions, in *The Global Carbon Cycle: Integrating Humans, Climate, and the Natural World*, edited by C. B. Field and M. R. Raupach, chap. The global carbon cycle: integrating humans, climate and the natural world, pp. 45–76, Island Press, Washington, D.C.

Gruber, N., D. Clement, B. R. Carter, R. A. Feely, S. van Heuven, M. Hoppema, M. Ishii, R. M. Key, A. Kozyr, S. K. Lauvset, C. Lo Monaco, J. T. Mathis, A. Murata, A. Olsen, F. F. Perez, C. L. Sabine, T. Tanhua, and R. Wanninkhof (2019), The oceanic sink for anthropogenic CO_2 from 1994 to 2007, *Science*, *363*(6432), 1193, doi:https://doi.org/10.1126/science.aau5153.

Hamme, R. C., P. W. Webley, W. R. Crawford, F. A. Whitney, M. D. DeGrandpre, S. R. Emerson, C. C. Eriksen, K. E. Giesbrecht, J. F. R. Gower, M. T. Kavanaugh, M. A. Peña, C. L. Sabine, S. D. Batten, L. A. Coogan, D. S. Grundle, and D. Lockwood (2010), Volcanic ash fuels anomalous plankton bloom in subarctic northeast pacific, *Geophysical Research Letters*, *37*(19), doi:https://doi.org/10.1029/2010GL044629.

Hansen, J., A. Lacis, R. Ruedy, and M. Sato (1992), Potential climate impact of Mount Pinatubo eruption, *Geophysical Research Letters*, *19*(2), 215–218, doi:https://doi.org/10.1029/91GL02788.

Holland, M. M., D. A. Bailey, B. P. Briegleb, B. Light, and E. Hunke (2012), Improved sea ice shortwave radiation physics in CCSM4: The impact of melt ponds and aerosols on Arctic sea ice, *J. Climate*, *25*(5), 1413–1430, doi:https://doi.org/10.1175/JCLI-D-11-00078.1.

Hunke, E. C., and W. H. Lipscomb (2008), CICE: the Los Alamos sea ice model user's manual, version 4, *Los Alamos Natl. Lab. Tech. Report*, *LA-CC-06-012*.

Hurrell, J. W., M. M. Holland, P. R. Gent, S. Ghan, J. E. Kay, P. J. Kushner, J. F. Lamarque, W. G. Large, D. Lawrence, K. Lindsay, W. H. Lipscomb, M. C. Long, N. Mahowald, D. R. Marsh, R. B. Neale, P. Rasch, S. Vavrus, M. Vertenstein, D. Bader, W. D. Collins, J. J. Hack, J. Kiehl, and S. Marshall (2013), The Community Earth System Model: A Framework for Collaborative Research, *B. Am. Meteorol. Soc.*, *94*(9), 1339–1360, doi:https://doi.org/10.1175/BAMS-D-12-00121.1.

Johnson, G. C., and N. Gruber (2007), Decadal water mass variations along 20°w in the Northeastern Atlantic Ocean, *Progress in Oceanography*, *73*(3), 277–295, doi:https://doi.org/10.1016/j.pocean.2006.03.022.

Kay, J. E., C. Deser, A. Phillips, A. Mai, C. Hannay, G. Strand, J. M. Arblaster, S. C. Bates, G. Danabasoglu, J. Edwards, M. Holland, P. Kushner, J. F. Lamarque, D. Lawrence, K. Lindsay, A. Middleton, E. Munoz, R. Neale, K. Oleson, L. Polvani, and M. Vertenstein (2015), The Community Earth System Model (CESM) Large Ensemble project: A community resource for studying climate change in the presence of internal climate variability, *B. Am. Meteorol. Soc.*, *96*(8), 1333–1349, doi:https://doi.org/10.1175/BAMS-D-13-00255.1.

Langman, O., P. Hanson, S. Carpenter, and H. YH (2010), Control of dissolved oxygen in northern temperate lakes over scales ranging from minutes to days, *Aquatic Biology*, *9*, 193–202, doi:https://doi.org/10.3354/ab00249.

Lauvset, S. K., N. Lange, T. Tanhua, H. C. Bittig, A. Olsen, A. Kozyr, S. Alin, M. Álvarez, K. Azetsu-Scott, L. Barbero, S. Becker, P. J. Brown, B. R. Carter, L. C. da Cunha, R. A. Feely, M. Hoppema, M. P. Humphreys, M. Ishii, E. Jeansson, L.-Q. Jiang, S. D. Jones, C. Lo Monaco, A. Murata, J. D. Müller, F. F. Pérez, B. Pfeil, C. Schirnick, R. Steinfeldt, T. Suzuki, B. Tilbrook, A. Ulfsbo, A. Velo, R. J. Woosley, and R. M. Key (2022), GLODAPv2.2022: the latest

version of the global interior ocean biogeochemical data product, *Earth System Science Data*, *14*, 5543–5572, doi:https://doi.org/10.5194/essd-14-5543-2022.

Lawrence, D. M., K. W. Oleson, M. G. Flanner, C. G. Fletcher, P. J. Lawrence, S. Levis, S. C. Swenson, and G. B. Bonan (2012), The CCSM4 land simulation, 1850–2005: Assessment of surface climate and new capabilities, *J. Climate*, *25*(7), 2240–2260, doi:https://doi.org/10.1175/JCLI-D-11-00103.1.

Lester, J. G., N. S. Lovenduski, H. D. Graven, M. C. Long, and K. Lindsay (2020), Internal variability dominates over externally forced ocean circulation changes seen through CFCs, *Geophys. Res. Lett.*, *47*, e2020GL087,585, doi: https://doi.org/10.1029/2020GL087585.

Macdonald, A. (2018), Cruise Report: SO4P, *Nathaniel B. Palmer*, *SO4P*(2018 MAR 09-2018 MAY 14), doi:https://cchdo.ucsd.edu/data/14272/320620180309$_d$*o.pdf*.

Macdonald, A., and S. Mecking (2015), Cruise Report: P16N, *Ronald H. Brown*, *P16N*(25 May 2015-27 June 2015), doi: https://cchdo.ucsd.edu/data/14283/33RO20150525$_d$*o.pdf*.

McKinley, G. A., A. R. Fay, Y. A. Eddebbar, L. Gloege, and N. S. Lovenduski (2020), External forcing explains recent decadal variability of the ocean carbon sink, *AGU Advances*, *1*(2), e2019AV000,149, doi:https://doi.org/10.1029/2019AV000149.

Milinski, S., N. Maher, and D. Olonscheck (2020), How large does a large ensemble need to be?, *Earth System Dynamics*, *11*(4), 885–901, doi: https://doi.org/10.5194/esd-11-885-2020.

Moore, J. K., K. Lindsay, S. C. Doney, M. C. Long, and K. Misumi (2013), Marine ecosystem dynamics and biogeochemical cycling in the Community Earth System Model [CESM1(BGC)]: Comparison of the 1990s with the 2090s under the RCP4.5 and RCP8.5 scenarios, *J. Climate*, *26*(23), 9291–9312, doi: https://doi.org/10.1175/JCLI-D-12-00566.1.

Robock, A. (2000), Volcanic eruptions and climate, *Reviews of Geophysics*, *38*(2), 191–219, doi:https://doi.org/10.1029/1998RG000054.

Rosenberg, M. (2006), Cruise Report: SO4I, *Aurora Australis*, *SO4I*(2006 JAN 02-2006 MAR 12), doi:https://cchdo.ucsd.edu/cruise/09AR20060102.

Sabine, C. L., R. A. Feely, F. J. Millero, A. G. Dickson, C. Langdon, S. Mecking, and D. Greeley (2008), Decadal changes in pacific carbon, *Journal of Geophysical Research: Oceans*, *113*(C7), doi:https://doi.org/10.1029/2007JC004577.

Sarmiento, J. L., and N. Gruber (2006), *Ocean Biogeochemical Dynamics*, Princeton University Press, Princeton, NJ, USA.

Schneider, D. P., C. M. Ammann, B. L. Otto-Bliesner, and D. S. Kaufman (2009), Climate response to large, high-latitude and low-latitude volcanic eruptions in the community climate system model, *Journal of Geophysical Research: Atmospheres*, *114*(D15), doi:https://doi.org/10.1029/2008JD011222.

Smith, R., P. Jones, B. Briegleb, F. Bryan, G. Danabasoglu, J. Dennis, J. Dukowicz, C. Eden, B. Fox-Kemper, P. Gent, M. Hecht, S. Jayne, M. Jochum, W. Large, K. Lindsay, M. Maltrud, N. Norton, S. Peacock, M. Vertenstein, and S. Yeager (2010), *The Parallel Ocean Program (POP) Reference Manual*, Los Alamos National Laboratory Tech. Rep. LAUR-10-01853, Los Alamos, NM.

Stenchikov, G., T. L. Delworth, V. Ramaswamy, R. J. Stouffer, A. Wittenberg, and F. Zeng (2009), Volcanic signals in oceans, *Journal of Geophysical Research: Atmospheres*, *114*(D16), doi:https://doi.org/10.1029/2008JD011673.

Talley, L. (2014), Cruise Report: P16S, *Nathaniel B. Palmer*, *P16S*(2014 Mar 20-2014 May 05), doi:https://cchdo.ucsd.edu/data/13738/p16s$_3$20620140320*do.pdf*.

Tanhua, T., D. W. Waugh, and J. L. Bullister (2013), Estimating changes in ocean ventilation from early 1990s CFC-12 and late 2000s SF6 measurements, *Geophysical Research Letters*, *40*(5), 927–932, doi:https://doi.org/10.1002/grl.50251.

Ting, Y.-H., and M. Holzer (2017), Decadal changes in southern ocean ventilation inferred from deconvolutions of repeat hydrographies, *Geophysical Research Letters*,

44(11), 5655–5664, doi:https://doi.org/10.1002/2017GL073788.

Wanninkhof, R., and L. Barbero (2014), Cruise Report: A16S, *Ronald H. Brown*, *A16S*(2013 DEC 23-2014 FEB 05), doi: https://cchdo.ucsd.edu/cruise/33RO20131223.

Wanninkhof, R., S. C. Doney, J. L. Bullister, N. M. Levine, M. Warner, and N. Gruber (2010), Detecting anthropogenic CO_2 changes in the interior Atlantic Ocean between 1989 and 2005, *J. Geophys. Res.*, *115*(C11), doi: https://doi.org/10.1029/2010JC006251.

Warner, M., and R. Weiss (1985), Solubilities of chlorofluorocarbons 11 and 12 in water and seawater, *Deep Sea Research Part A. Oceanographic Research Papers*, *32*(12), 1485–1497, doi:https://doi.org/10.1016/0198-0149(85)90099-8.

Waugh, D. W., F. Primeau, T. DeVries, and M. Holzer (2013), Recent Changes in the Ventilation of the Southern Oceans, *Science*, *339*(6119), 568–570, doi: https://doi.org/10.1126/science.1225411.

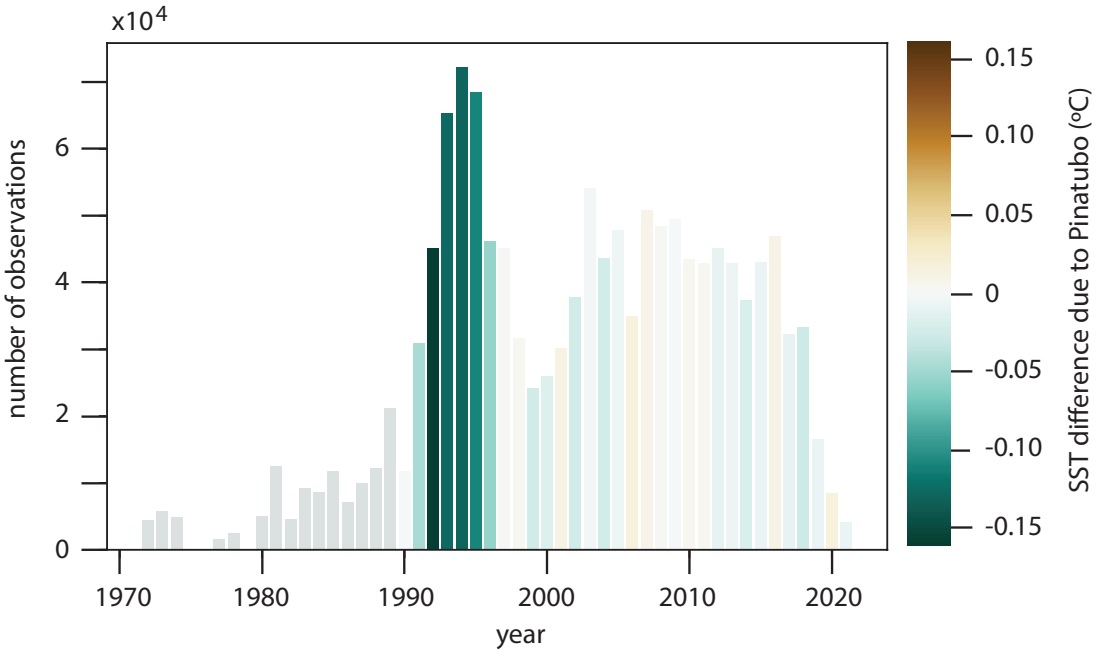

Figure 1. Temporal evolution of the number of ocean biogeochemical observations collected from hydrographic cruises over 1972-2021 [*Lauvset et al.*, 2022]. Bars are shaded according to the Pinatubo-driven global sea surface temperature (SST) anomaly (°C), calculated as the difference in ensemble mean sea surface temperature between the LENS and NoPin ensembles.

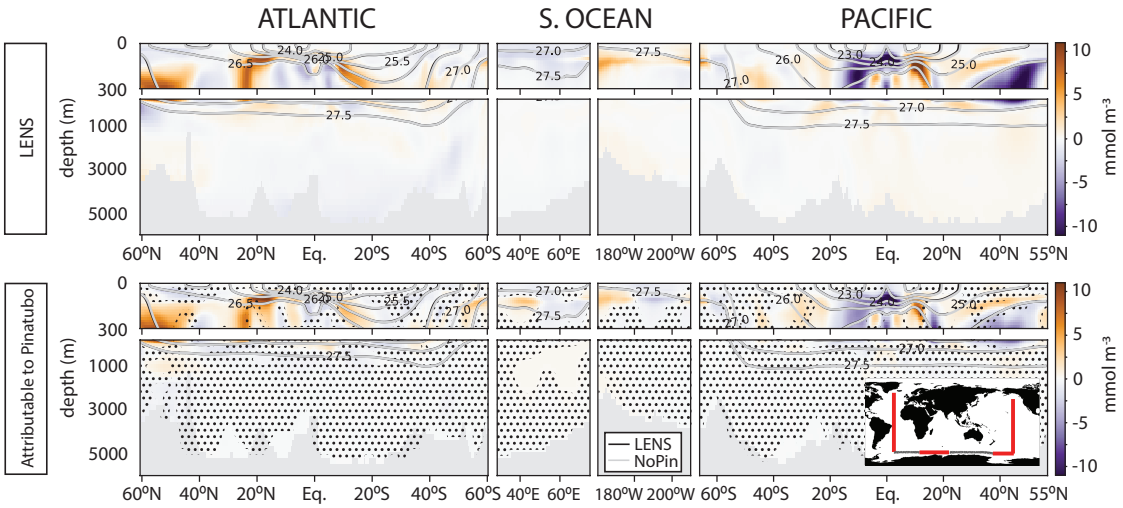

Figure 2. Externally forced, decadal change in apparent oxygen utilization (AOU; mmol m^{-3}) from 1993 to 2003 along the cruise paths shown in map inset. (top) Decadal change in the LENS ensemble mean AOU, and (lower) decadal change attributable to Pinatubo, estimated as the difference in the decadal changes between the LENS and NoPin ensemble means. Ensemble mean potential density contours (kg m^{-3}) in 2003 for LENS (NoPin) are shown in black (gray). Hatching indicates where Pinatubo-driven changes are not significant at the 95% confidence level [*Deser et al.*, 2012].

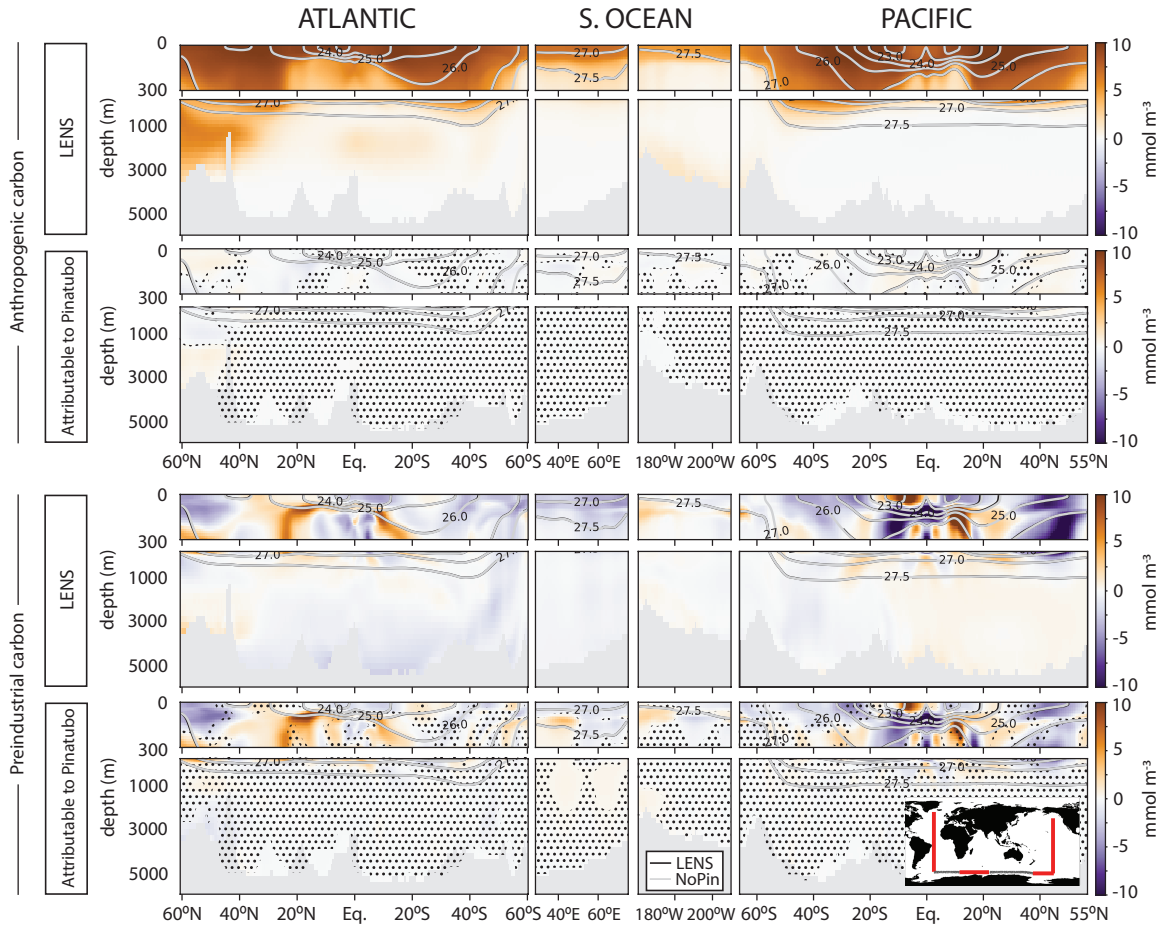

Figure 3. Externally forced, decadal change in (top two rows) anthropogenic and (bottom two rows) preindustrial carbon (mmol m^{-3}) from 1993 to 2003 along the cruise paths shown in map inset. (top and third) Decadal change in the LENS ensemble mean anthropogenic carbon, and (second and bottom) decadal change attributable to Pinatubo, estimated as the difference in the decadal changes between the LENS and NoPin ensemble means. Ensemble mean potential density contours (kg m^{-3}) in 2003 for LENS (NoPin) are shown in black (gray). Hatching indicates where Pinatubo-driven differences are not significant at the 95% confidence level [*Deser et al.*, 2012].

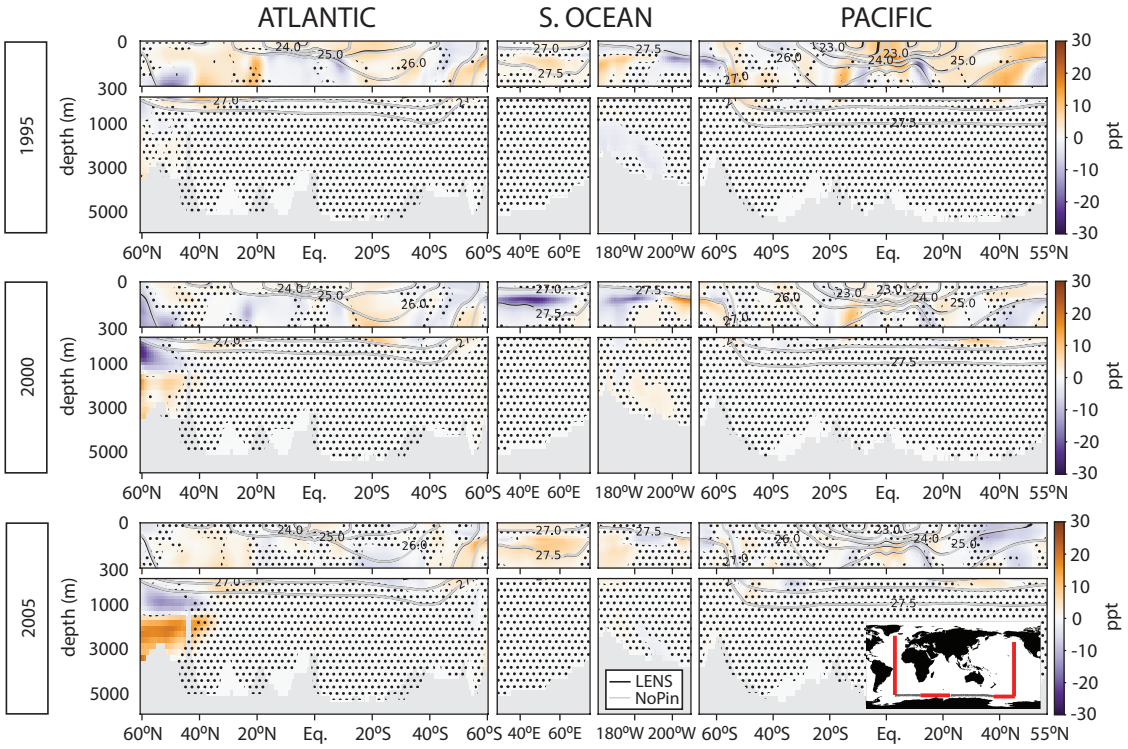

Figure 4. Pinatubo-driven difference in annual mean pCFC-12 (parts per trillion, ppt) in (top) 1995, (middle) 2000, and (bottom) 2005 along the cruise paths shown in map inset, estimated as the difference between the LENS and NoPin ensemble means. Ensemble mean potential density contours (kg m^{-3}) for the corresponding years in LENS (NoPin) are shown in black (gray). Hatching indicates where Pinatubo-driven forced differences are not significant at the 95% confidence level [*Deser et al.*, 2012].

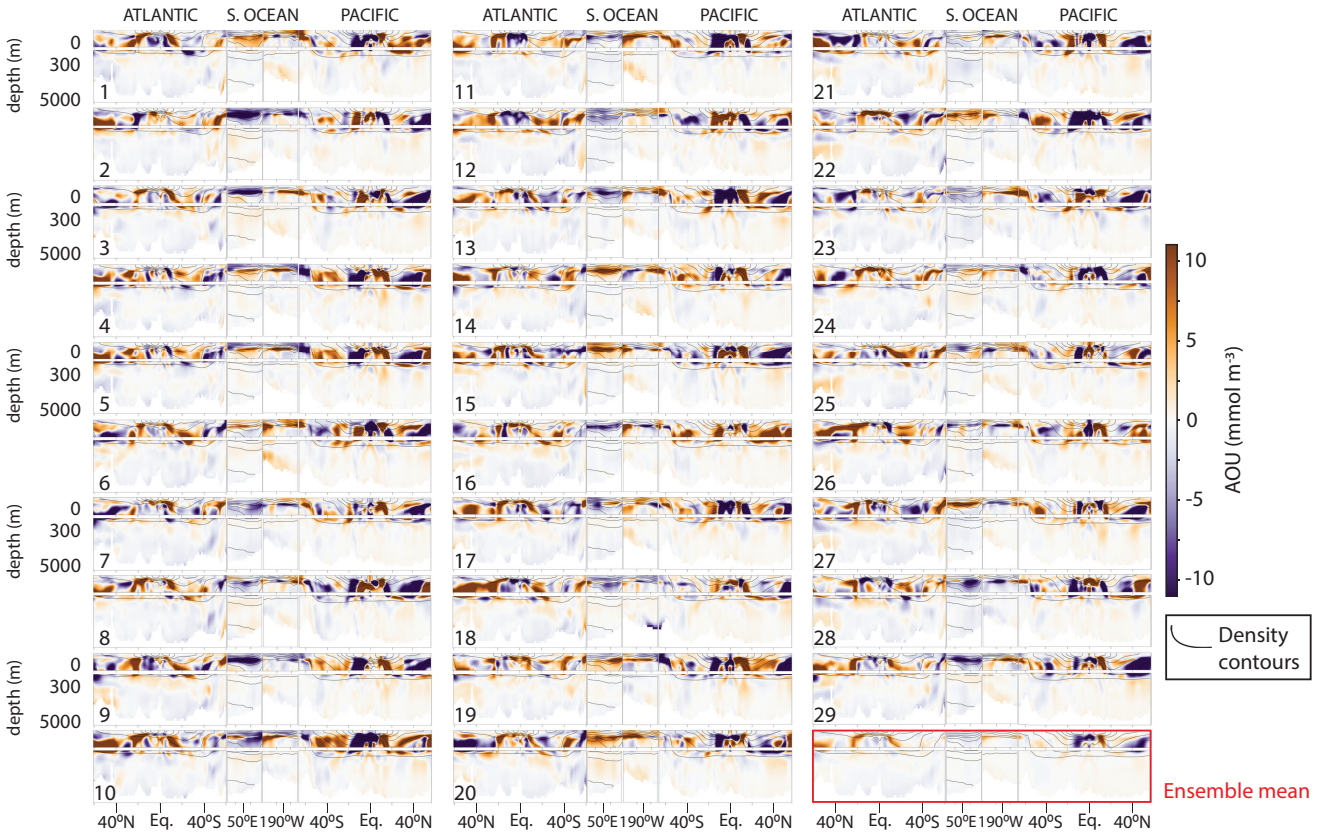

Figure S1. Externally driven, decadal change in apparent oxygen utilization (AOU; mmol m^{-3}) from 1993 to 2003 along the cruise paths shown in Figure 2 map inset. (top to bottom) Decadal change in LENS ensemble members 1-29. Lower right corner is the LENS ensemble mean decadal change, as shown in Figure 2. Ensemble mean potential density contours (kg m^{-3}) in 2003 for LENS (NoPin) are shown in black (gray).

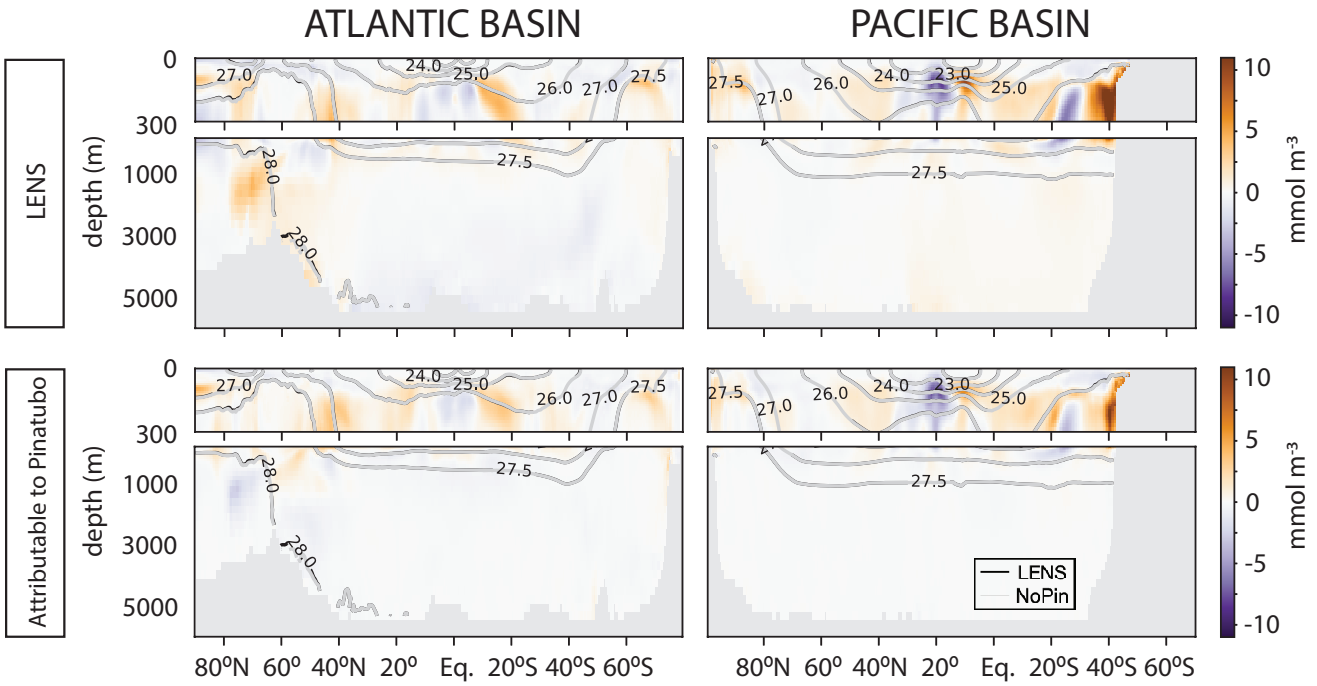

Figure S2. Pinatubo-driven difference in annual mean, zonal-mean apparent oxygen utilization (AOU; mmol m^{-3}) (LENS minus NoPin ensemble means) in the (left) Atlantic and (right) Pacific basins from 1993 to 2003. Ensemble mean potential density contours (kg m^{-3}) for the corresponding years in LENS (NoPin) are shown in black (gray).

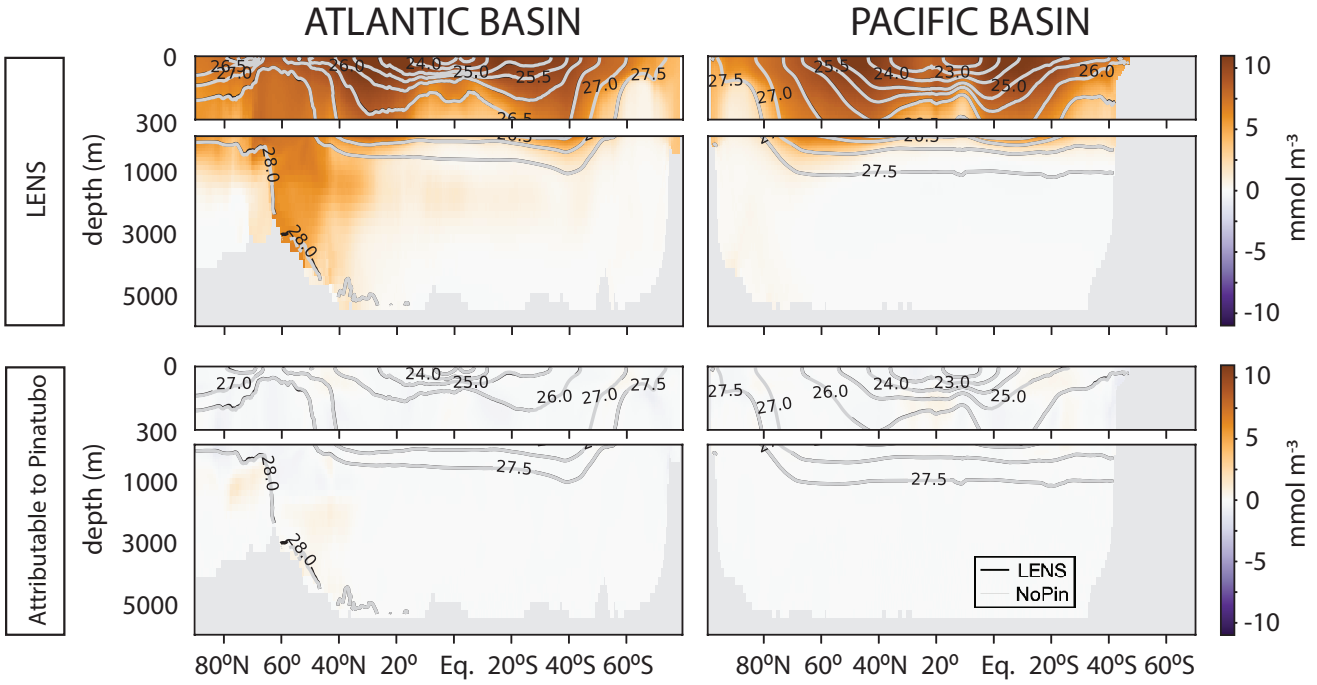

Figure S3. Pinatubo-driven difference in annual mean, zonal-mean anthropogenic carbon (mmol m^{-3}) (LENS minus NoPin ensemble means) in the (left) Atlantic and (right) Pacific basins from 1993 to 2003. Ensemble mean potential density contours (kg m^{-3}) for the corresponding years in LENS (NoPin) are shown in black (gray).

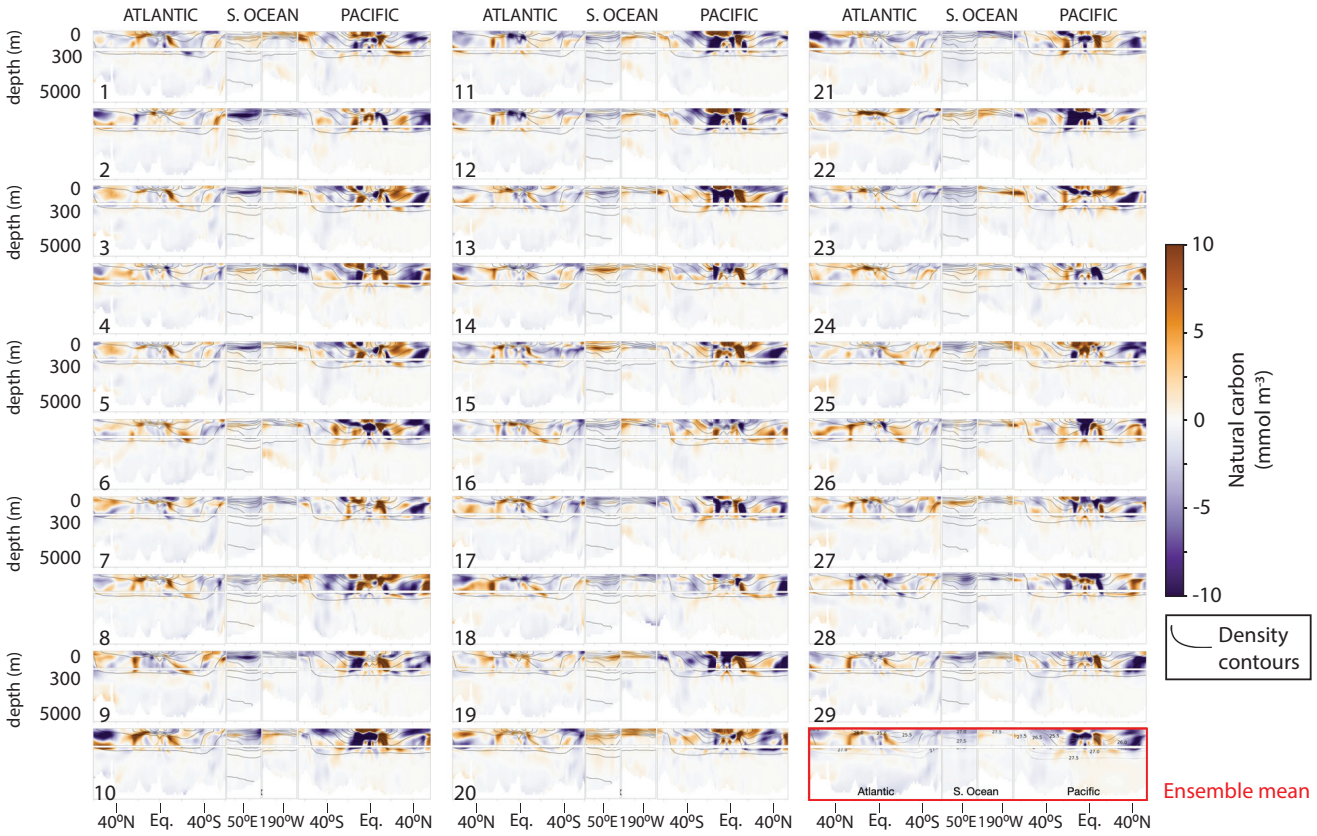

Figure S4. Externally forced, decadal change in preindustrial carbon (mmol m^{-3}) from 1993 to 2003 along the cruise paths shown in 3 map inset. (left to right) Decadal change in LENS ensemble members 1-29. Lower right corner is the LENS ensemble mean decadal change as shown in Figure 3. Ensemble mean potential density contours (kg m^{-3}) in 2003 for LENS (NoPin) are shown in black (gray).

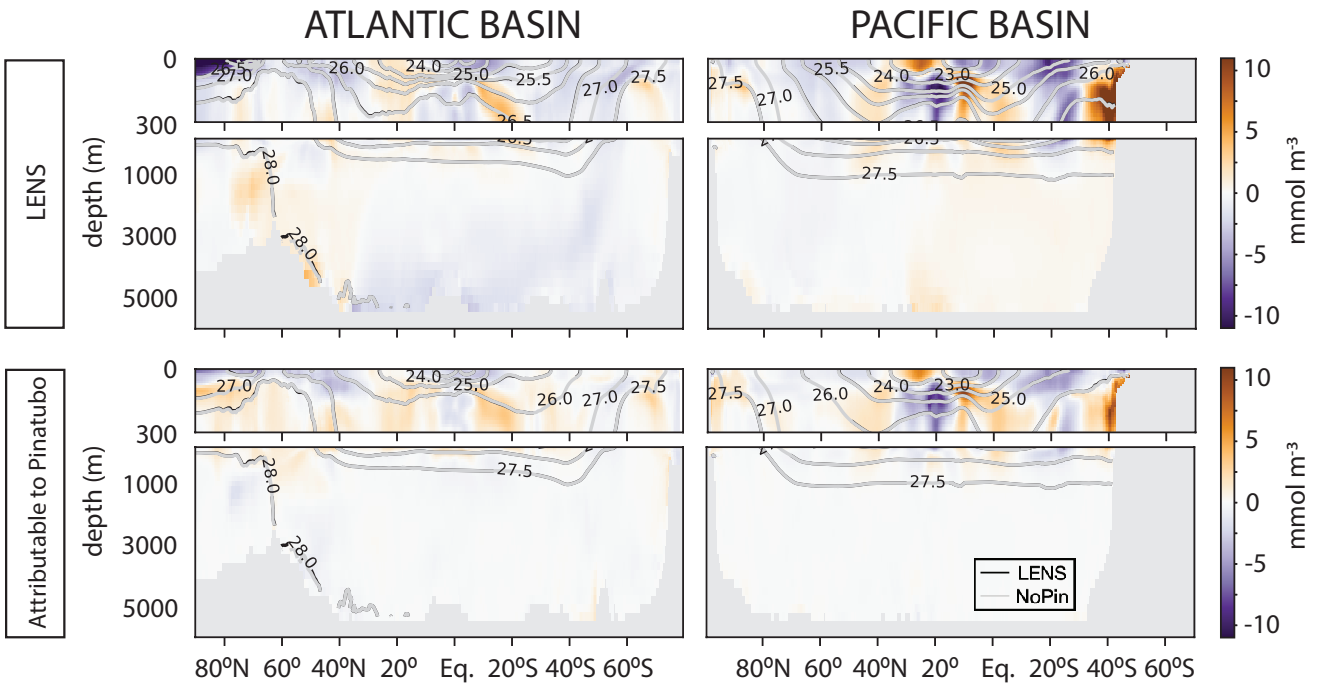

Figure S5. Pinatubo-driven difference in annual mean, zonal-mean preindustrial carbon (mmol m^{-3}) (LENS minus NoPin ensemble means) in the (left) Atlantic and (right) Pacific basins from 1993 to 2003. Ensemble mean potential density contours (kg m^{-3}) for the corresponding years in LENS (NoPin) are shown in black (gray).

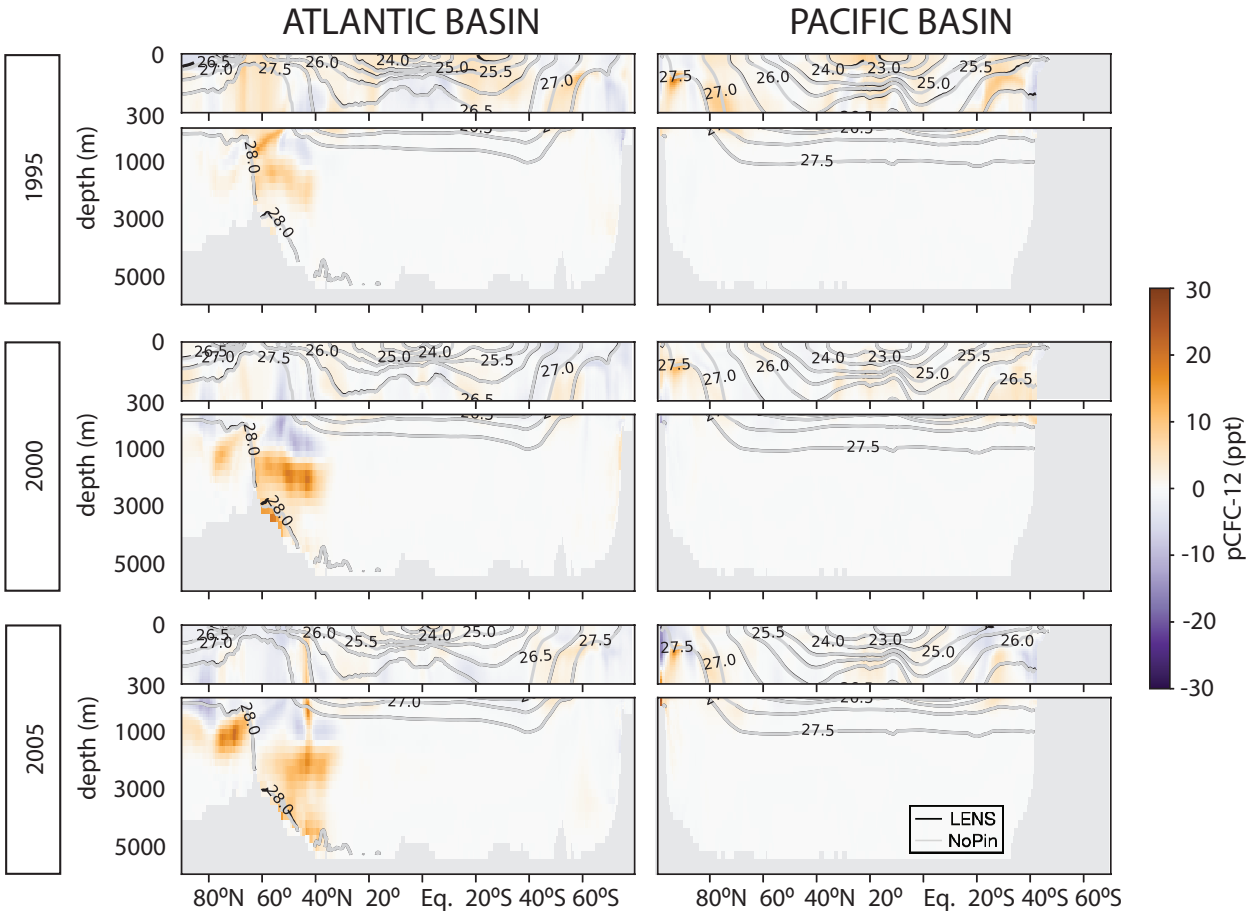

Figure S6. Pinatubo-driven difference in annual mean, zonal-mean pCFC-12 (ppt) (LENS minus NoPin ensemble means) in the (left) Atlantic and (right) Pacific basins in (top) 1995, (middle) 2000, and (lower) 2005. Ensemble mean potential density contours (kg m^{-3}) for the corresponding years in LENS (NoPin) are shown in black (gray).

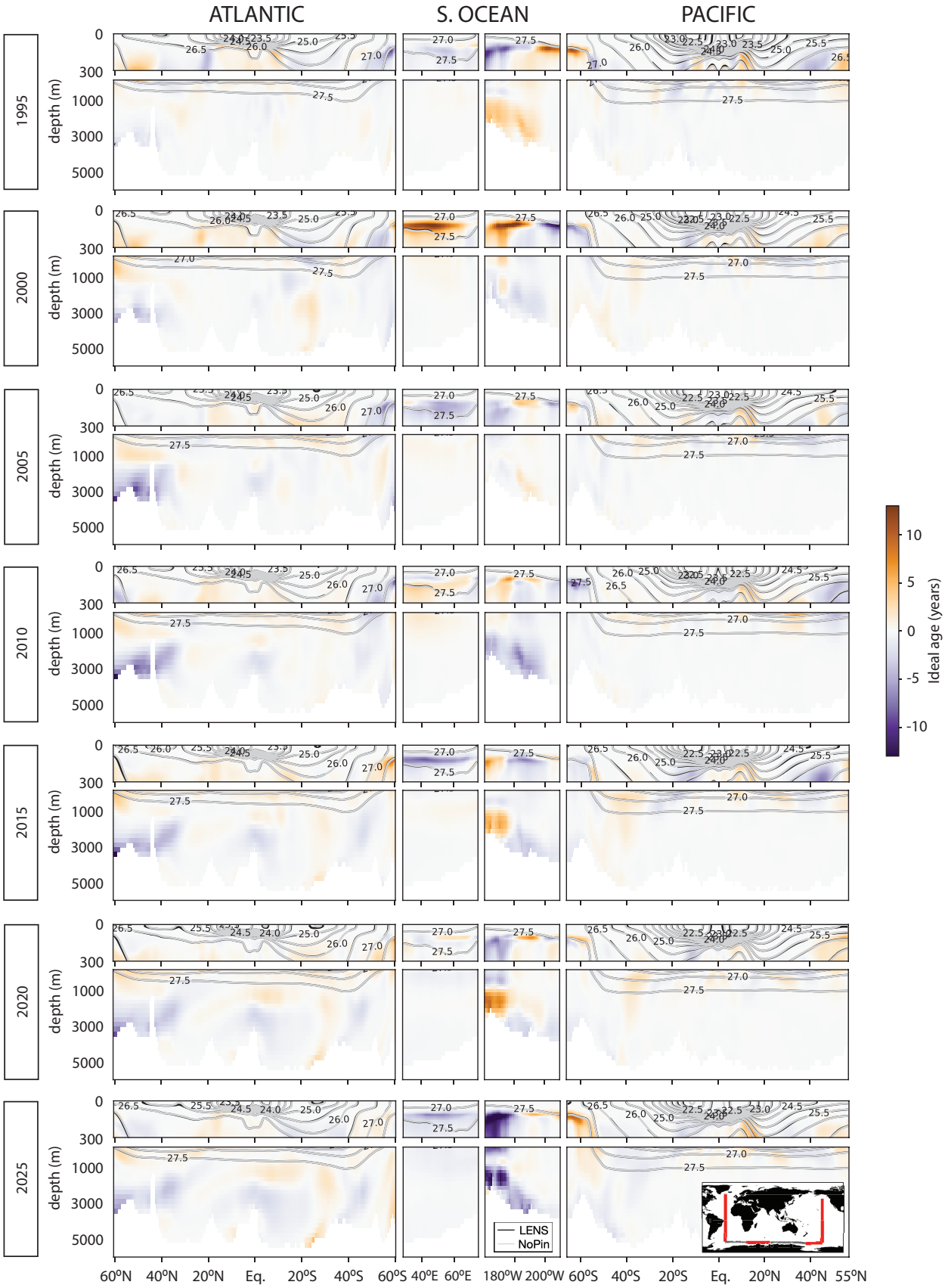

Figure S7. Pinatubo-driven difference in annual mean ideal age (years) (LENS minus NoPin ensemble means) from 1995 to 2025 in 5-year intervals along the cruise paths shown in map inset. Ensemble mean potential density contours (kg m^{-3}) for the corresponding years in LENS (NoPin) are shown in black (gray).

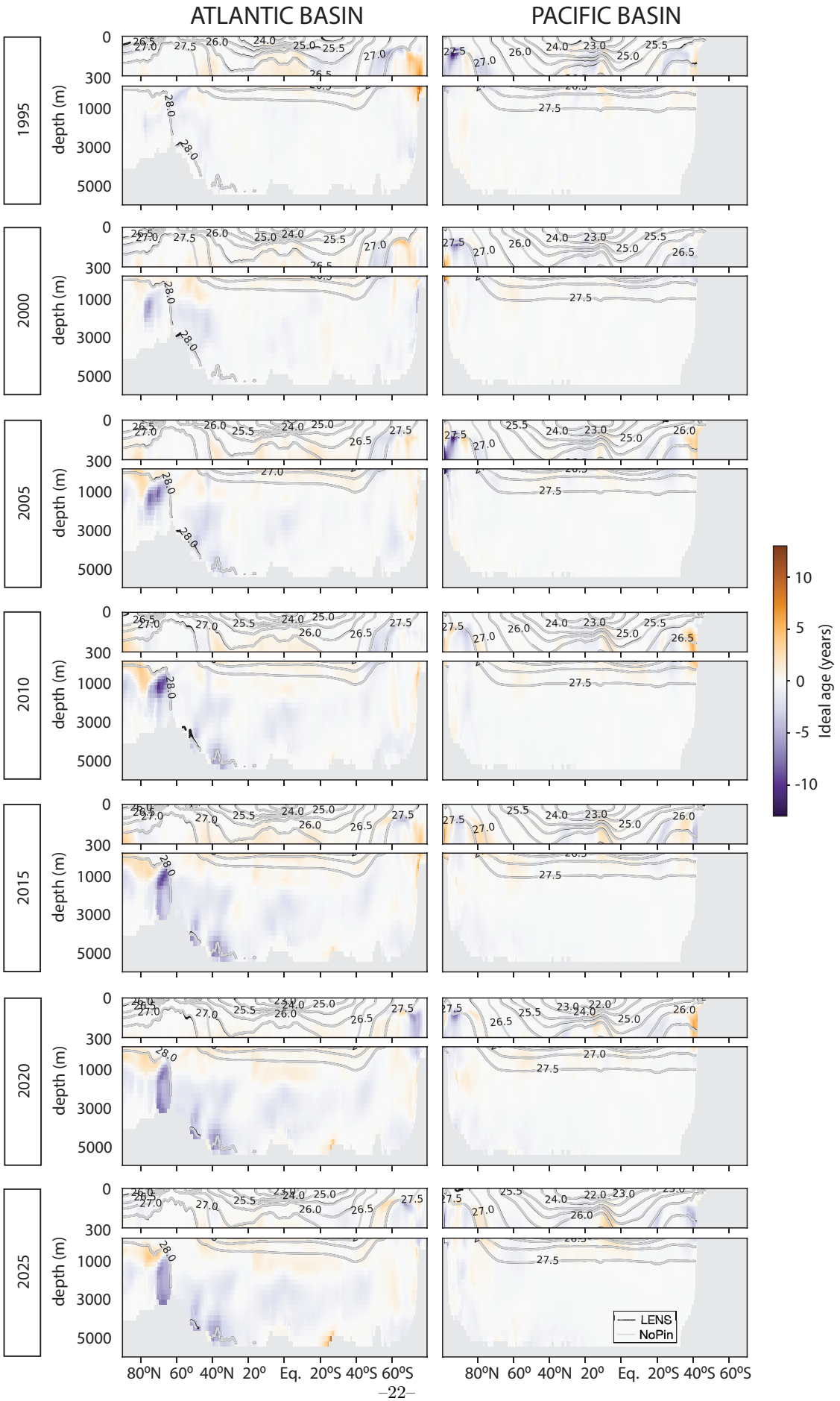

Figure S8. Pinatubo-driven difference in annual mean, zonal mean ideal age (years; LENS minus NoPin ensemble means) in the (left) Atlantic and (right) Pacific basins from 1995 to 2025 in 5-year intervals. Ensemble mean potential density contours (kg m^{-3}) for the corresponding years in LENS (NoPin) are shown in black (gray).